

Optimization of Silt Pit Dimensions and the Water Supply Period in Oil Palm Plantation by Artificial Neural Network Estimation

Husam Hasan Abdulaali^{1*}, Christopher Teh Boon Sung², Ali H. Abdulaali³,
Md Rowshon Kamal⁴, and Roslan Ismail²

1 Department of Soil science and Water Resources, Faculty of Agriculture, University of Basrah, Iraq

2 Department of Land Management, Faculty of Agriculture, Universiti Putra Malaysia, Selangor, Malaysia.

3 Department of Mechanical Engineering, College of Engineering, University of Basrah, Iraq

4 Department of Biological and Agricultural Engineering, Faculty of Engineering, Universiti Putra Malaysia, Selangor, Malaysia.

*Corresponding author: husam.abdulaali@uobasrah.edu.iq

Received: June 29, 2018; 1st Revised: January 5, 2019; Accepted: August 20, 2019

Abstract

Constructing a silt pit is one of the most widely adopted and effective practices used in oil palm plantations to conserve soil and water. The objective of this study was to utilize the HYDRUS-2D/3D to determine the optimal dimensions of silt pit and optimise the simulation results employing the multiple linear regression (MLR) and/or artificial neural network (ANN). Both methods were used to select the optimal size and dimensions of silt pit sizes depending on the amount of rain and soil properties. The treatments that were adopted included: 1) seven soil textures, 2) five surface slopes, and 3) three silt pits sizes. Each silt pit size comprised of three depth levels to accommodate the amount of water available in the pit. The approach first utilised the HYDRUS-2D/3D software to simulate the time-to-empty (TTE) of various silt pit sizes on different soil and slopes. Secondly, trends were then distinguished from the data, and the best fit was determined using MLR and ANN models to estimate the optimal silt pit size. The TTE was affected by the water head in the pits (H), pit width (W), the amount of water applied (Vw), and the pit volume (Vp), but was not affected by the surface slope (Slope). The findings demonstrated that the MLR models did not perform sufficiently to represent the results of TTE ($R^2 = 0.632$; $MSE = 85.83$) compared with the ANN models ($R^2 = 0.977$; $MSE = 10.33$). This was mainly due to the non-linear relations of these factors. The results demonstrated that by using the same input data, the ANN models could favourably be used for TTE predictions.

Keywords: Soil water conservation; Silt pit; HYDRUS-2D/3D; Multiple Linear Regression; Artificial Neural Network

1. Introduction

Water harvesting can be defined as a process that allows the collection of rainwater or surface runoff, which is then utilised for agricultural (for crops and vegetables) and domestic purposes, or for livestock watering. Soil management for soil fertility and rainwater harvesting can reduce the risk of nutrient depletion

(Giller *et al.*, 2006; Mupangwa *et al.*, 2006; Tiftonell *et al.*, 2007; Vanlauwe and Giller, 2006). It has been predicted that the rainwater harvesting processes could decrease the risk for crop failure and could help in improving soil fertility (Rockstrom, 2000). Improved soil fertility could decrease the nutrient loss and ensure the redistribution of the eroded nutrients in the soil (Bohluli *et al.*, 2014).

Studies have shown that the growth of healthy oil palm correlates significantly to high yield production which can be achieved through the application and optimisation of water management practices (Lim *et al.*, 2012; Bohluli *et al.*, 2014). There are many ways for conserving water and soil on steep slopes, one of which is by constructing terraces. Terraces may be defined as ground embankments constructed across the slope down to the lower surface runoff point in order to guide the run-off to the outlet at a stable velocity to prevent erosion, via the shortest path (Morgan, 2005).

In some regions, water run-off and soil erosion could be very severe, despite the construction of terraces or water conservatories. In these areas, the silt pits must be dug for reducing the water flow, which increases water infiltration in the soil and maximises water conservation (Afandi *et al.*, 2017; Murtillaksono *et al.*, 2007). Terminologies such as silt pit, pit/pitting, irrigation pit, diking/dammer-diker, water harvesting pit, and planting pit have been used to describe the straddling of contour trenches both in size and shape. All apply the same concepts to collect the run-off, trap and settle the sediment, thereby increasing soil moisture, improving the groundwater, breaking the slope length, reducing soil erosion and loss of fertiliser (Haridas, 2005; Bohluli *et al.*, 2014). Atmaja (2007) assessed the efficiency of constructing silt pits and ridge terraces for conserving the soil moisture content during the palm oil plantation. The researchers noted the highest soil water content in the areas containing silt pits. Furthermore, the researchers concluded that the silt pits could fulfil the water demand of the palm oil plants and thus, lead to increased production. However, there is no standard size for a silt pit, as the sizes vary depending on the soil properties, slope surface, and rainfall intensity. Since using direct measurement is time-consuming and costly, indirect methods have been developed such as numerical methods to estimate water flow and the transportation of nutrients. Moreover, modelling is used to assess soil properties such as the percentage of soil particles and/or water flow parameters. Notwithstanding, numerical

models are increasingly being used as an approach for predicting or analysing water flow and contaminant transport processes. One of the most prominent methods is the HYDRUS model.

HYDRUS-2D/3D (Karandish & Šimůnek, 2016; Šimůnek *et al.*, 2008) refers to software which is used for simulating transient, 2- or 3-D movement of the runoff water and soil nutrients for various boundary conditions, like irregular boundaries, and soil heterogeneities. The HYDRUS-2D/3D models can be used for many applications since these models are developed using simple input parameters that could be determined in the projects having limited resources (Karandish and Šimůnek, 2016). Notably, many studies have used a simulation approach (e.g., Rocha *et al.*, 2006; Warrick and Lazarovitch, 2007; Lazarovitch *et al.*, 2009), whereas, a number of other studies have used HYDRUS (2D/3D) to calibrate and test the predictions against experimental data (e.g., Abbasi *et al.*, 2003a,b; Wöhling and Schmitz, 2007; Crevoisier *et al.*, 2008; Zerihun *et al.*, 2014). Accordingly, this provides confidence that the model can adequately describe these complex systems.

Some recent studies have used neural networks for classification, simulation and optimisation of some models applied in the field of engineering science (Menhaj 2000). Many researchers have applied neural networks models for estimating the infiltration rates (Jain and Kumar, 2006), exchangeable cations (Amini *et al.*, 2005), saturated hydraulic conductivity (Schaap *et al.*, 2001; Doae *et al.*, 2005; Parasuraman *et al.*, 2006; Ghanbarian-Alavijeh *et al.*, 2010), and hydrologic processes (Lazarovitch *et al.*, 2009; Isik *et al.*, 2013). One of the more recent studies by (Elnesr and Alazba, 2017) compared the HYDRUS-2D/3D results with an ANN to simulate water distribution under a surface dripper. The researchers noted that the ANN prediction models could provide good results, with the correlation coefficient values for the 7809 data points ranging between 0.93 and 0.99.

The primary aim of this research was to construct a HYDRUS-2D/3D model to predict the optimum size of the silt pit by quantifying and examining the relationships between the

silt pit sizes with the soil types, steepness/slope, and rainfall intensities (volume of water in the pits) based on the large number of treatments as mentioned earlier. Notably, this was to distinguish the trend of all experimental elements used in the study. Furthermore, the secondary objective of this research was to obtain a quick and low-cost analytical procedure to estimate the optimal size of the silt pit for the maximum time-to-empty (TTE) prediction. It is aimed to find an alternative of using the complicated numerical programme like HYDRUS-2D/3D model, we will utilise ANN with the aid MLR analysis to perform the task.

2. Methodology

2.1. Numerical methods

The first stage of this study utilises the software HYDRUS 2D/3D models to simulate the time-to-empty of various silt pit sizes on different soils, water head, and slopes. The governing equations and initial boundary conditions for transient flow are described along with providing a brief introduction on the numerical methods for transient water flow. The Richards equation is the dominant equation applied in unsteady conditions and is shown in 2D mode (Equation 1) (Azhdari, 2008; Simunek et al., 2005). The HYDRUS model is used to solve Richard’s analysis using a linear finite element model (FEM), to simulate the movement of water in the soil (Abassi, 2005).

$$\frac{\partial \theta}{\partial t} = \frac{\partial}{\partial x_i} \left[K \left(K_{ij}^A \frac{\partial h}{\partial x_j} + K_{iz}^A \right) \right] - S \quad (1)$$

where θ is the volumetric moisture; K is the unsaturated hydraulic conductivity; h is the matrix potential; S is the water intake by root; α is the angle between the flow path and vertical axis; x is the distance; and t is the time.

Table 1. Shows silt pit sizes with different dimensions

Silt pit size (m ³)	Silt Pit Dimensions (m)		
	Depth (D)	Width (W)	Length (L)
3	0.50	1.50	4.00
	0.75	1.00	4.00
	1.00	0.75	4.00
4	0.50	2.00	4.00
	0.75	1.33	4.00
	1.00	1.00	4.00
5	0.50	2.50	4.00
	0.75	1.67	4.00
	1.00	1.25	4.00

2.2. Numerical experiment factors

In this study, seven soils with wide-ranging soil textures (sand, sandy loam, loam, silt, sandy clay loam, silty clay, and clay) were used based on the soil hydraulic properties according to the USDA classification. Five surface slopes (0°, 5°, 10°, 15°, 20°, and 25°) were employed. Three silt pits of sizes (3, 4, and 5 m³) were used where each size consisted of three depth levels (D1, D2, and D3). The length (L) was fixed for all sizes (4 m) (Table 1). Next, a two dimensional (2D) model was generated using HYDRUS with the W (width) and D (depth) of the silt pits, (Figure 1). The volumes of water applied in the pits (volume of water runoff that is generated during a rainfall storm of the catchment area) were 1, 2, 3, 4, and 5 m³ respectively.

Figure 1 illustrates the initial and boundary conditions, flow domain, and the prescribed boundary conditions. The simulated domain was 600 cm deep and 600 cm wide. The transport domain was discretised into 3,953 to 5,506 2D-elements with a fine grid formed around the silt pit walls of (5.5 cm), with the element spacing gradually increasing farther from the silt pit walls until reaching the global targeted size of the finite elements (21 cm). A time-variable flux boundary condition was specified around the silt pit wall. Notably, during water applications, a variable water head is calculated depending on the flux discharge rate. The atmosphere boundary condition was found to be negligent at the soil surface (no flux). Also, a free drainage boundary condition was specified at the bottom boundary and vertical sides, allowing for downward drainage. The initial soil water contents were equally applied to the field capacity. The TTE of water in the pit was determined by monitoring the cumulative amount of water flux from the walls of the pit (variable head boundary) as well as the time until obtaining the volume of water in the silt pit.

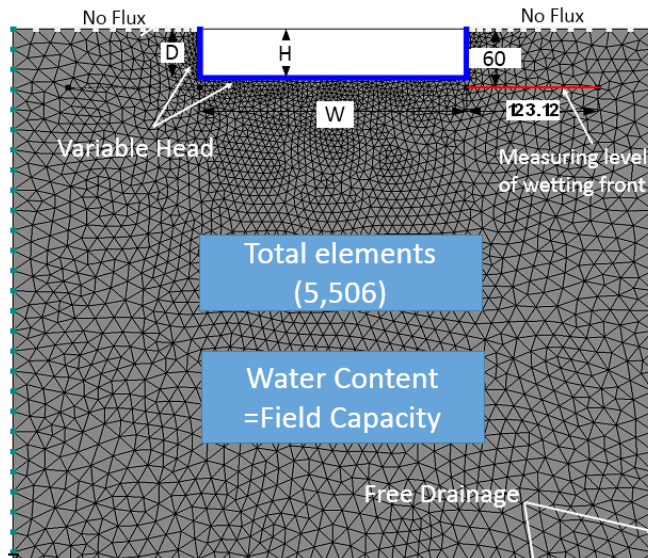


Figure 1: Screen capture of the geometry figure generated from the HYDRUS 2D/3D window to show how the initial and boundary conditions were applied

2.3. Multiple linear regression

MLR is a linear regression model, which can be applied for analysing the relationship between a single response variable (dependent variable) and 2-or more controlled variables (independent variables). MLR analysis is generally used for describing the quantitative relationship between the response variables and multiple explanatory variables (Tabari *et al.*, 2012). The following linear equation is used in the MLR models:

$$Y = \alpha_0 + \alpha_1x_1 + \alpha_2x_2 + \dots + \alpha_nx_n \quad (2)$$

where Y is the dependent variable, α_0 and α_n are the MLR parameters, and x_1 and x_n are the independent variables.

2.4. Neural networks model Design

An ANN model is an interconnected network comprising of several simple processing units known as neurons, similar to the biological neurons present in a human brain. There is an interconnection between these layers where each has a magnification weight. The architecture of the multi-hidden layers neural network is illustrated in Figure 2 (Rojas, 2013).

Five variables Sand%, Clay%, V_w/W , Slope, and V_p were used as independent variables (input of ANN), and one dependent variable TTE will also be used (output of ANN).

Therefore, each input vector will consist of 5 numbers, and the output consists of only one number. Some researchers stated that only one hidden layer is necessary for such cases (Akbar *et al.*, 2018). Other researchers have found that using two hidden layers provides the best results (Kavuncuoglu *et al.*, 2018). This will be checked later in the study using trials. Also, a milestone, “2n”, “2n+1” has been suggested by some researchers (Park, 2011) to determine the number of neurons in a single hidden layer where n represents the input layer nodes number (independent variables).

There are many activation functions used by researchers, while in practice just a small number are familiar. Some examples are the hyperbolic tangent sigmoidal, log-sigmoidal, and some trigonometric and linear functions (Rojas, 2013). After conducting several trials, a logarithmic sigmoid function for hidden neurons and linear function for output neurons was determined to be the most acceptable for the prediction of TTE.

Regarding the training process of the network, it begins with the weights being initialised randomly in an interval [-1, 1]. Next, there must an iterative training algorithm to minimise the cost function. All training algorithms sometimes fall in local and not global points. Notably, no algorithm can be

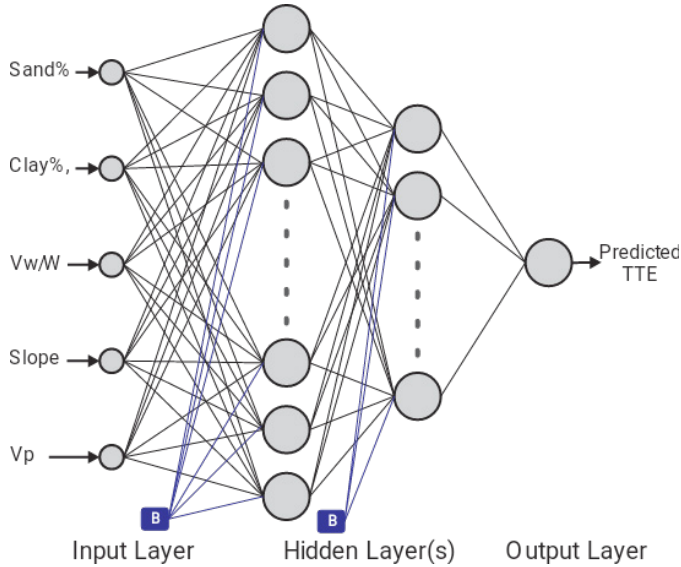


Figure 2: Schematic of the ANN architecture, showing highly interconnected nodes (neurons)

assured of achieving the global optimum in non-linear problems (Gopalakrishnan, 2010). Most of the training algorithms attempt to solve the problem with suitable weights, which are sensitive to initial weight assumptions such as back-propagation (Rojas, 2013).

Four training algorithms were used in this paper to determine which one is optimum for the study. These included;

resilient back propagation (RP), Levenberg-Marquardt (LM), scaled conjugate gradient (SCG), and Bayesian regulation (BR) (Gopalakrishnan, 2010). A comparison of the different algorithms was carried out based on the mean squared error. Data were normalised before submitting to the networks. This process limits the highest and lowest values to certain intervals such as [-1, 1] or [0, 1].

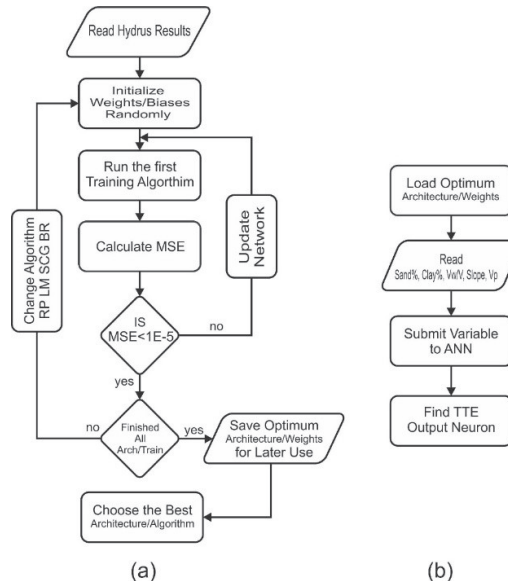


Figure 3: Proposed Procedure for ANN Model for Regression: (a) Training and determining the optimum ANN (b) Later used for the trained ANN

The submitted data set is divided into three subsets to implement an acceptable stopping technique; training, validation, and test sets. Measuring the predictive capability of the model is checked by the test set. Here, we constrained the total number of iterations (epochs) to 1000, and the validation is stopped when the errors increased for 50 epochs (due to the large dataset). In this research, 1512 datasets were divided as 70 % training, 15 % validation, and 15 % test sets of the total data. MATLAB software randomly made the selection of these sets. Next, different network hierarchies and different training algorithms were trained using these data to determine the optimum networks and optimum training algorithm. Figure 3a illustrates the proposed method for determining the best ANN for the prediction of TTE. While Figure 3b displays how the optimum network will be used by MATLAB at a later stage.

2.5. Model Performance Measurement

For evaluating the proposed neural network model, statistical parameters like the correlation coefficient (R^2) and Mean Square Error (MSE) (small MSE value reflects a proper training of the model) were used and were estimated as follows:

$$R^2 = \frac{\sum_{i=1}^n (O_i - O_{ave})(P_i - P_{ave})}{\sqrt{\sum_{i=1}^n (O_i - O_{ave})^2 (P_i - P_{ave})^2}} \quad (3)$$

$$MSE = \frac{1}{N} \sum_{i=1}^N (O_i - P_i)^2 \quad (4)$$

where O_i are the observed values; P_i is the predicted values; O_{ave} is the measured rate values; N is the comparison numbers; P_{ave} is the simulated values. The Root mean squared error (RMSE) is the square root of MSE.

3. Results and Discussion

3.1. Trend Study

HYDRUS displayed all soil textures having the same trend (Figure 4). Hence, the average of all soils was taken to understand the effect of the silt pit dimensions, the volume of water in the pit, volume of the pit, and the slope surface on the TTE.

Figure 5 illustrates the effect of the water head (H), the volume of the silt pit (V_p), and depth of the pit (D) on the TTE with different surface slopes. In this Figure, fixing V_p and increasing H will cause the TTE to decrease. To explain this, V_p 5 m³ is selected with two depths: D3 (W = 125 cm and D = 100 cm) and D1 (W = 250 m and D = 50 cm), as shown in Figure 6a and b, respectively. The wetted area (wetted side areas and base area) of pit

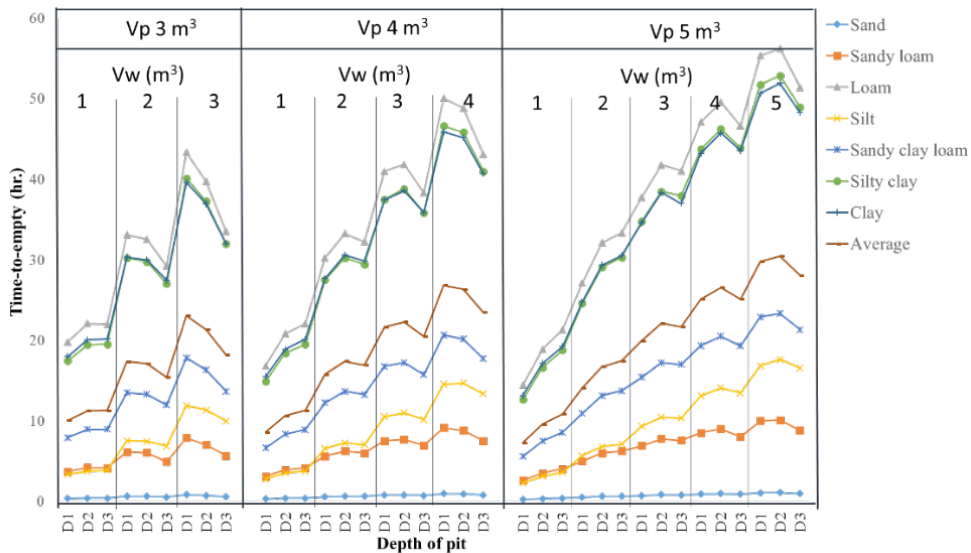


Figure 4: Shows the effect of soil textures to time-to-empty (TTE) with all experimental elements. [volume of pits (V_p), volume of water (V_w), and depth of pits (D1, D2, and D3 are 50, 75, 100 cm, respectively)]

D3 (12.5 m²) is larger than the wetted area of pit D1 (11.5 m²). Therefore, this means that more significant amounts of water would be in contact with the soil; thus, leading to much larger water flow. Moreover, the head of water in the silt pit D1 (50 cm) is half that of D3 (100 cm). Accordingly, this will lead to an increase of the pressure head and increase the water flow from the wetted area as shown in Equation (12) (Kale & Sahoo, 2011):

$$f(t) = K \left(1 + \frac{ho + hs}{L} \right) \quad (12)$$

where $f(t)$ is the infiltration rate; K is effective hydraulic conductivity; ho is the depth of ponding water over the soil surface; hs represents the capillary suction head at the wetting front; L is the depth of wetting front below the bottom of the pond.

Figure 5 also illustrates that when H is fixed, and W is gradually increased, this will increase TTE. Indeed, this can be explained in Figure 6; the amount of water in the silt pit with wider wall dimensions (water volume will be 5 m³) (Figure 6a) is double that of the pit with narrow dimensions (water volume will be 2.5 m³) (Figure 6c). This then leads to the continuous release of water for much of the period. Also, Figure 5 illustrates that there is no effect shown by the slopes to TTE for all experimental elements. The reason for this may be caused by the set of the initial water conditions equal to the field capacity in the HYDRUS geometry.

3.2 Performance of ANN model on the prediction task

In this study, a three- and four-layered ANN (which have 1 and 2 Hidden layers respectively) with different hidden layers and nodes were used for the prediction of TTE. Figure 7 shows the relationship between the network structures versus the mean squared error for different training

algorithms for a network with the single hidden layer. The same calculations were performed for the networks with double hidden layers (i.e. 400 networks tested with 4 training algorithms) (Figure 7). The utilised model showed that the single hidden layer provides reasonable prediction results. The designed networks contain different types of activation functions; logarithmic sigmoid for the hidden layer(s) and pure linear function for the output layer. Table 2 displays the optimal ANN having the LM training algorithm with logarithmic sigmoid as a transfer function in the hidden layer with the structure 5-20-1. Whereas, the optimum double hidden layer network has the structure of 5-7-3-1 trained by BR. It is clear from observing the image sketches in the figure that the darker blue areas have less MSE. Therefore, taking this into account, the number of weights to be updated, and the values of R^2 and MSE, the optimal function will be considered as 5-7-3-1.

3.3 Performance of MLR model

Based on the TTE data collected from the simulation, a linear model was next found from the relation between the dependent model and the five independent variables (Sand%, Clay%, V_w/V , Slope, and V_p). The model was obtained using the least squares method, and the results acquired as given in Equation (5):

$$TTE (HR) = -6.334 - 0.135 Sand\% + 0.513 Clay\% + 4.568 \frac{V_w}{W} - 0.426 Slope + 2.498 V_p \quad (5)$$

As observed in Figure 8, the modelled TTE values were not in agreement with the actual values. The values of R^2 and MSE are 0.632 and 85.83, respectively. Therefore, the MLR model results are not suitable for this prediction. Accordingly, it is important to search for a nonlinear fitting model for the predictions.

Table 2. Optimum Values of the Single and Double Hidden Layers Networks

Layers	Structure	Activation Functions	R ²	MSE	RMSE	Algorithm
1	5-20-1	logsimoid-Linear	0.976	11.1	3.33	LM
2	5-7-3-1	Logsimoid-logsimoid-Linear	0.978	8.9	2.98	BR

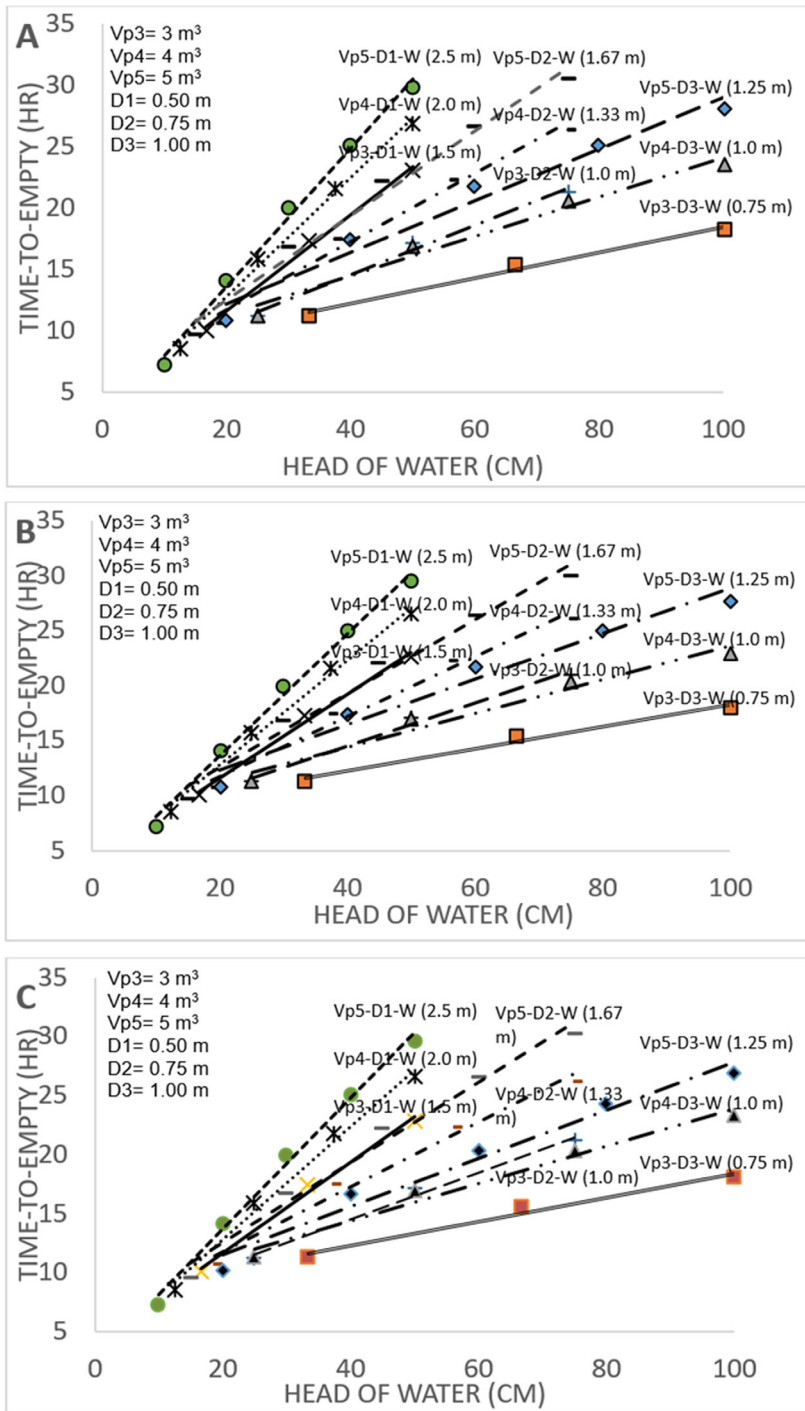


Figure 5. Effect of head of water in pits (H), volume of pits (Vp), width of pits (W), and depth of pits (D) to time-to-empty. A slope surface 0°, B slope surface 15°, and C slope surface 25°

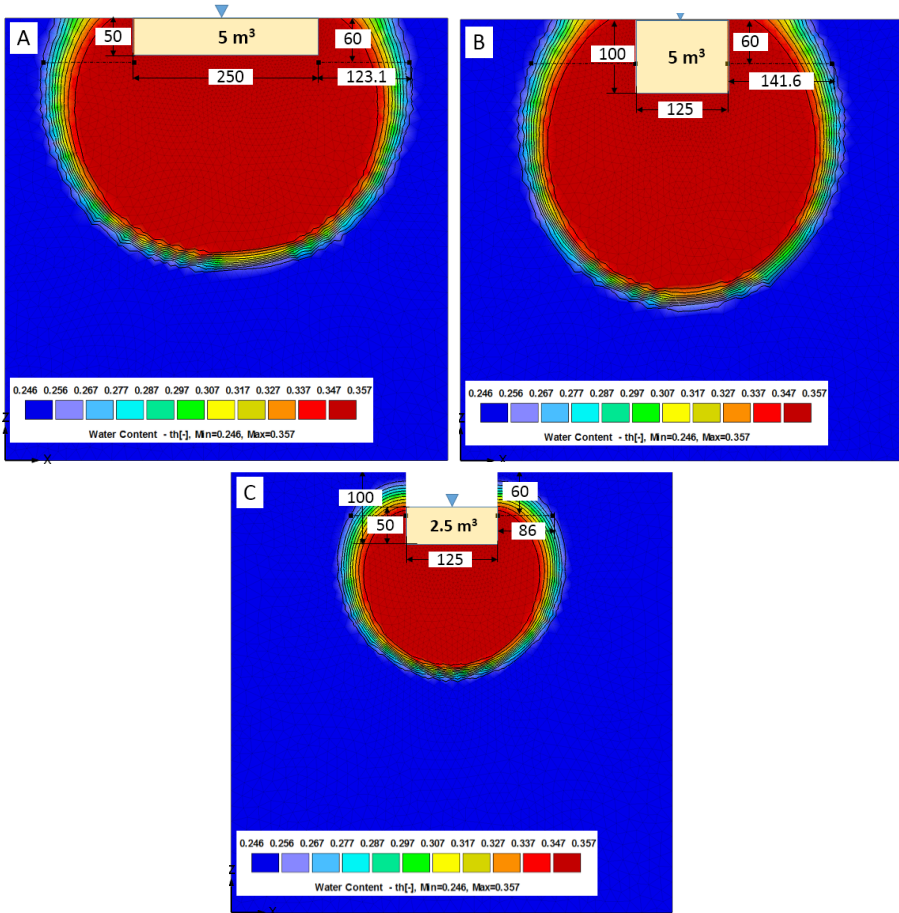


Figure 6. Show the effect of depth (D) and width (W) of the pit in each of the same volume of pit (V_p) and amount of water (V_w) (A and B) and in the same value of head of water (H) and different size of pit (V_p) (A and C) (Screen capture of HYDRUS window results)

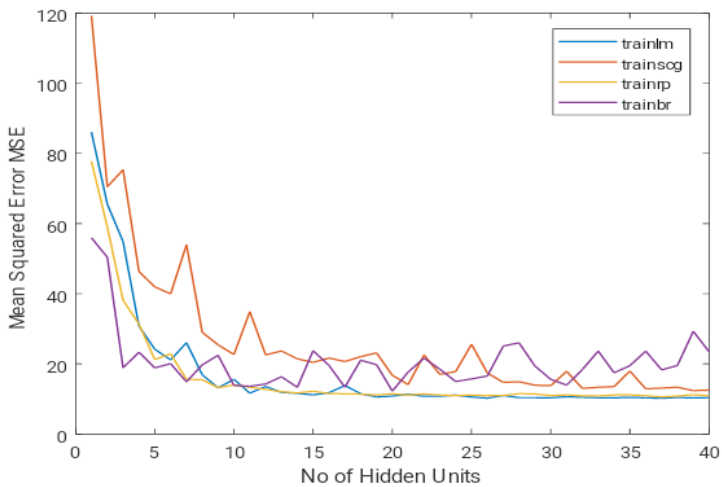


Figure 7. Optimum Single Hidden Layer ANN

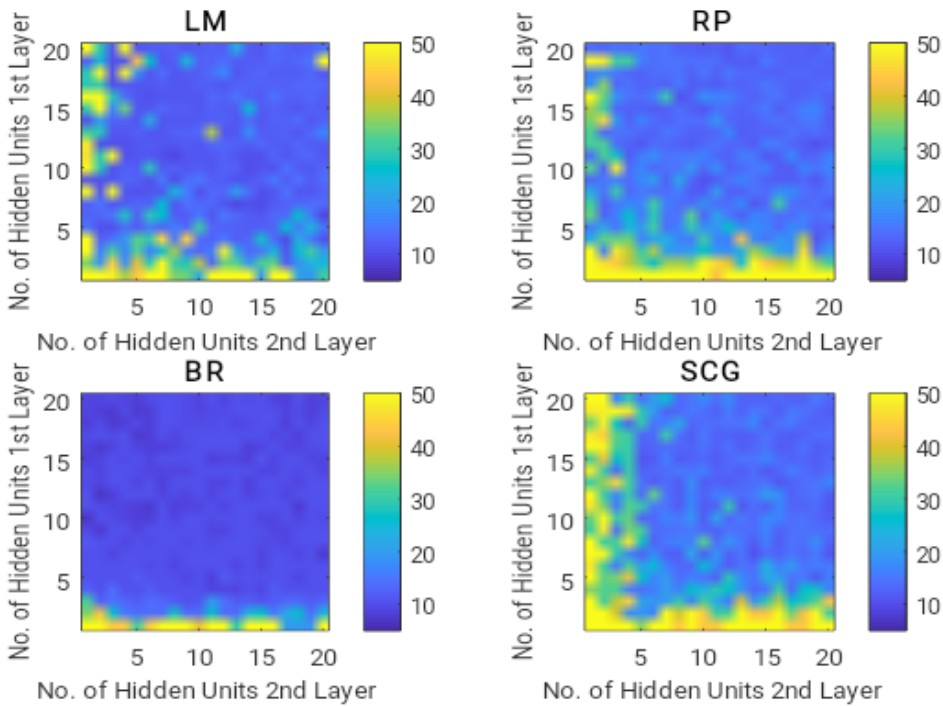


Figure 8: Image plots for MSE vs. number of hidden neurons for Double Hidden Layer ANN

3.4 Comparison between the ANN and MLR models

The HYDRUS results were considered as the true or measured values (or target values). The best way of viewing the fitting results is by drawing the relation between the fitted and actual data (i.e. it must be on a line of the slope equal to 1 intercepting the y-axis at the origin). If this result is displayed like a line, then they

are considered to be the best fit. By examining the performance results of the MLR and ANN (5-7-3-1, Logsig-Logsig-Purelin, BR) models, the MSE and R^2 values are 10.33 and 0.977 for ANN and 85.83 and 0.632 for MLR (Figure 9), respectively. The results show that the ANN models might be built to predict TTE which is better than the MLR model. This can be validated by observing the histogram illustrated in Figure 10.

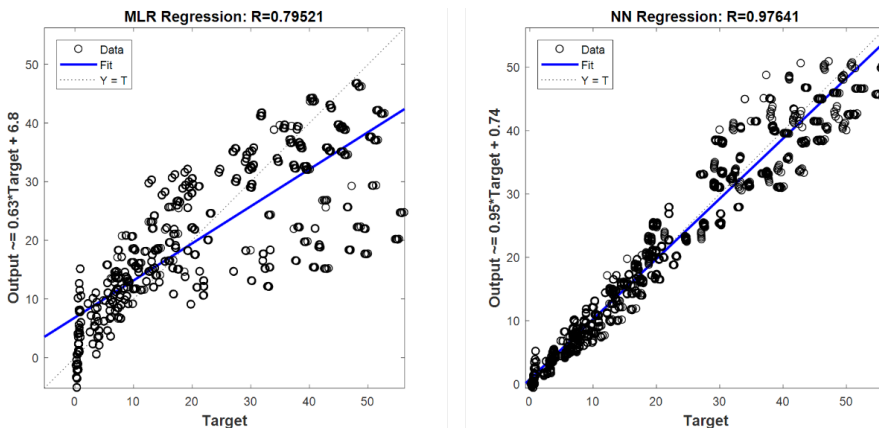


Figure 9: Correlation between the actual results (Targets) and predicted results by MLR Model (left) and ANN Model with Double hidden layers of structure 5-7-3-1 (right)

As shown in Figure 11, a correlation can be observed between the predicted and actual variables. As a result, the neural networks models can precisely predict the TTE and is therefore considered as a useful tool for this area of application.

The ANNs prediction models based on our view will play a vital role in the applications and techniques for modelling a more complicated problem for soil modelling, especially in the experimental field. However, one disadvantage of the ANN prediction model is that it requires a large observation set for the training process and must cover the entire prediction range.

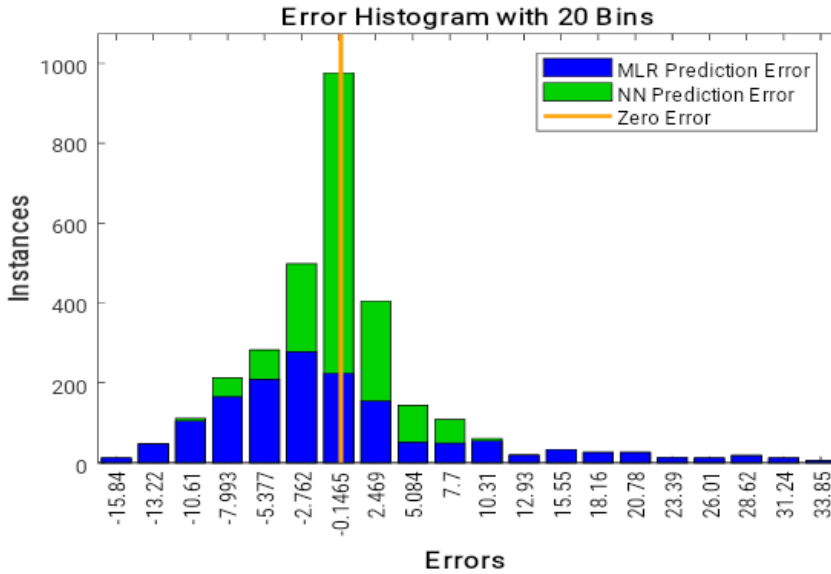


Figure 10: Error Occurrence Histogram for all 1512 Points

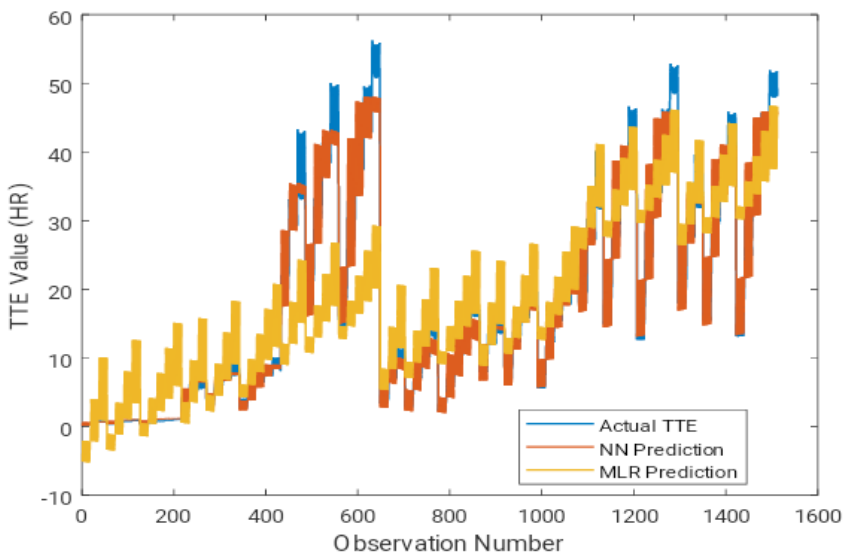


Figure 11: Prediction of trained ANN 5-7-3-1 vs MLR Predictions and Actual results

4. Conclusions

From the results using HYDRUS 2D/3D, the trend of the results indicated that when increasing the head of water in the silt pit, the TTE will decrease. Moreover, the depth of the silt pit could not be lower than the active root zone of the oil palm trees. In other words, in an area with limited rainfall, the depth of the silt pit should be shallow enough to avoid the possibility of water redistribution under the root zone of the oil palm tree.

This paper has aimed to develop ANN and MLR models to predict the TTE in silt pits employing five variables, Sand%, Clay%, Vw/W, Slope, and Vp. Statistical analyses were carried out to compare both models. The results indicated that the ANN model is an effective model for predicting the TTE especially in the presence of using complex linearities. A closer correlation was observed between the predicted values from the model and those found by using HYDRUS 2D/3D. Therefore, designers can rely on the TTE obtained from the model without the need to restore the complex simulation based on the available information such as soil texture (Clay and Sand %). Moreover, the amount of water generated from the rainfall in catchment area could be used to determine the suitable TTE for any plant field. Further research into this field is necessary before obtaining a definitive model(s) for the predictions. Future work may be performed using experimental data instead of using simulation data. Additionally, applicants can follow the steps illustrated in Figure 3 for the prediction. Full details of data used and MATLAB codes for this paper are found in the project page: <https://github.com/Husam78/SiltPit>.

Acknowledgement

The authors wish to thank Prof Jirka Simunek from the Department of Environmental Sciences, University of California Riverside, USA, and Dr Rudiyanto from the Department of Civil and Environmental Engineering, Bogor Agricultural University, Indonesia, for their help with the numerical inversion methods using the HYDRUS 2D/3D software.

References

- Abassi F. Simulation of water movement in soil using HYDRUSID model. [Training workshop on modeling in irrigation and drainage]. Irrigation and Drainage national committee, 2005.
- Abbasi F, Jacques D, Šimůnek J, Feyen J, Genuchten MT. Inverse estimation of soil hydraulic and solute transport parameters from transient field experiments: Heterogeneous soil. *Transactions of the ASAE* 2003a; 46: 1097–1111.
- Abbasi F, Simunek J, Feyen J, Van Genuchten M T, Shouse P. Simultaneous inverse estimation of soil hydraulic and solute transport parameters from transient field experiments: Homogeneous soil. *Transactions of the ASAE* 2003b; 46(4): 1085–1095.
- Afandi A M, Zuraidah Y, Nurzuhaili H A, Zulkifli H, Yaqin M. Managing soil deterioration and erosion under oil palm. *Oil Palm Bulletin* 2017; 75: 1-10.
- Akbar A, Kuanar A, Patnaik J, Mishra A, Nayak S. Application of Artificial Neural Network modeling for optimization and prediction of essential oil yield in turmeric (*Curcuma longa* L.). *Computers and Electronics in Agriculture* 2018; 148: 160-178.
- Amini M, Abbaspour KC, Khademi H, Fathianpour N, Afyuni M, Schulin R. Neural network models to predict cation exchange capacity in arid regions of Iran. *European Journal of Soil Science* 2005; 56(4): 551-559.
- Atmaja H. Soil moisture contents in soil conservation technique of ridge terrace and silt pit in oil palm plantation PTPN VII Rejosari, Lampung. Land Study Program Land Influmining and Land Resources. Faculty of Agriculture, Bogor. 2007.
- Azhdari KH. Simulation of moisture distribution in soil under drip irrigation system using HYDRUS-2D model, *Journal of Agricultural Sciences and Natural Resources* 2008; 15(1): 168-180.
- Bohluli M, Teh BSC, Hanif AHM, Rahman ZA. Silt pit efficiency in conserving soil water as simulated by HYDRUS 2D model. *Pertanika Journal of Tropical Agricultural Science* 2014; 37(3).

- Crevoisier D, Popova Z, Mailhol J C, Ruelle P. Assessment and simulation of water and nitrogen transfer under furrow irrigation. *Agricultural Water Management* 2008; 95(4): 354-366.
- Doace M, Sharestani M S, Bagheri F. Modeling saturated hydraulic conductivity in clay soils in guilan province (Iran) using artificial neural networks. *Journal Agricultural Science* 2005, 1:41-48 (In Persian).
- Elnesr M, Alazba A. Simulation of water distribution under surface dripper using artificial neural networks. *Computers and Electronics in Agriculture* 2017; 143: 90-99.
- Ghanbarian-Alavijeh B, Liaghat A, Sohrabi S. Estimating saturated hydraulic conductivity from soil physical properties using neural networks model. *World Academy of Science, Engineering and Technology* 2010; 4: 108-113.
- Giller KE, Misiko M, Tittonell PA. Managing organic resources for soil amendment. *LEISA: ILEIA Newsletter for Low-External-Input and Sustainable Agriculture* 2006; 22(4): 16-17.
- Gopalakrishnan K. Effect of training algorithms on neural networks aided pavement diagnosis. *International Journal of Engineering, Science and Technology* 2010; 2(2): 83-92.
- Haridas, V. *Soil and Water Conservation Measure*. New Delhi: CBCI Centre Ashok Place, Goleadakkana. 2005.
- Isik S, Kalin L, Schoonover J E, Srivastava P, Lockaby B G. Modeling effects of changing land use/cover on daily streamflow: An Artificial Neural Network and curve number based hybrid approach. *Journal of Hydrology* 2013; 485: 103-112.
- Jain A, Kumar A. An evaluation of artificial neural network technique for the determination of infiltration model parameters. *Applied Soft Computing* 2006; 6(3): 272-282.
- Kale RV, Sahoo B. Green-Ampt infiltration models for varied field conditions: A revisit. *Water Resources Management* 2011; 25(14): 3505.
- Karandish F, Šimůnek J. A comparison of numerical and machine-learning modeling of soil water content with limited input data. *Journal of Hydrology* 2016; 543: 892-909.
- Kavuncuoglu H, Kavuncuoglu E, Karatas S M, Benli B, Sagdic O, Yalcin H. Prediction of the antimicrobial activity of walnut (*Juglans regia* L.) kernel aqueous extracts using artificial neural network and multiple linear regression. *Journal of Microbiological Methods* 2018; 148: 78-86.
- Lazarovitch N, Poulton M, Furman A, Warrick A. Water distribution under trickle irrigation predicted using artificial neural networks. *Journal of Engineering Mathematics* 2009; 64(2): 207-218.
- Lazarovitch N, Warrick A, Furman A, Zerihun D. Subsurface water distribution from furrows described by moment analyses. *Journal of Irrigation and Drainage Engineering* 2009; 135(1): 7-12.
- Lim K, Lim S, Parish F, Suharto R. *RSPO manual on best management practices (BMPs) for existing oil palm cultivation on peat*. RSPO, Kuala Lumpur. 2012.
- Menhaj M. *Fundamental of artificial neural network*. Tehran: Amir kabir University Publishing; 2000. (in Persian)
- Morgan R. *Soil Erosion and Conservation*. Oxford: Blackwell Publishing ; 2005.
- Mupangwa W, Love D, Twomlow S. Soil-water conservation and rainwater harvesting strategies in the semi-arid Mzingwane Catchment, Limpopo Basin, Zimbabwe. *Physics and Chemistry of the Earth* 2006; Parts A/B/C, 31(15-16): 893-900.
- Murtillaksono K, Siregar H, Darnosarkoro W. Model neraca air di perkebunan kelapa sawit (water balance model in oil palm plantation). *Juournal Penelitian Kelapa Sawit* 2007: 14(2); 21-36.
- Parasuraman K, Elshorbagy A, Si BC. Estimating saturated hydraulic conductivity in spatially variable fields using neural network ensembles. *Soil Science Society of America Journal* 2006; 70(6): 1851-1859.

- Park HI. Study for application of Artificial Neural Networks in geotechnical problems. In: Hui CLP, editor. *Artificial Neural Networks-Application*. Intech, Available from: <https://www.intechopen.com/books/artificial-neural-networks-application/study-for-application-of-artificial-neural-networks-in-geotechnical-problems>
- Rocha D, Abbasi F, Feyen J. Sensitivity analysis of soil hydraulic properties on subsurface water flow in furrows. *Journal of Irrigation and Drainage Engineering* 2006; 132(4): 418-424.
- Rockstrom J. Water resources management in smallholder farms in Eastern and Southern Africa: An overview. *Physics and Chemistry of the Earth* 2000, Part B: Hydrology, Oceans and Atmosphere 25(3): 275-283.
- Rojas R. *Neural networks: A systematic introduction*. Berlin: Springer Science & Business Media; 2013.
- Schaap MG, Leij FJ, Van Genuchten M T. Rosetta: A computer program for estimating soil hydraulic parameters with hierarchical pedotransfer functions. *Journal of Hydrology* 2001; 251(3-4): 163-176.
- Simunek J, Van Genuchten M T, Sejna M. The HYDRUS-1D software package for simulating the one-dimensional movement of water, heat, and multiple solutes in variably-saturated media. [Research Reports: Version 3] Department of environmental sciences, University of California riverside, Riverside, California, 2005.
- Šimunek J, van Genuchten M T, Šejna M. Development and applications of the HYDRUS and STANMOD software packages and related codes. *Vadose Zone Journal* 2008; 7(2): 587-600.
- Tabari H, Kisi O, Ezani A, Talaei PH. SVM, ANFIS, regression and climate based models for reference evapotranspiration modeling using limited climatic data in a semi-arid highland environment. *Journal of Hydrology* 2012; 444: 78-89.
- Tittonell P, Zingore S, Van Wijk MT, Corbeels M, Giller KE. Nutrient use efficiencies and crop responses to N, P and manure applications in Zimbabwean soils: Exploring management strategies across soil fertility gradients. *Field Crops Research* 2007; 100(2-3): 348-368.
- Vanlauwe B, Giller KE. Popular myths around soil fertility management in sub-Saharan Africa. *Agriculture, Ecosystems and Environment* 2006; 116(1-2): 34-46.
- Warrick A, Lazarovitch N. Infiltration from a strip source. *Water Resources Research* 2007; 43(3): 299-303.
- Wöhling T, Schmitz GH. A physically based coupled model for simulating 1D surface–2D subsurface flow and plant water uptake in irrigation furrows. I: Model development. *Journal of Irrigation and Drainage Engineering* | 2007, 133:538–547. Available from: doi:10.1061/(ASCE)0733-9437(2007)133:6(538).
- Zerihun D, Sanchez C, Lazarovitch N, Warrick A, Clemmens A, Bautista E. Modeling flow and solute transport in irrigation furrows. *Irrigation Drainage System Engineering* 2014; 3(2):1-16.